ELSEVIER

Chemical Physics 242 (1999) 177–193

Chemical Physics

Energy gradient method for the ground, excited, ionized, and electron-attached states calculated by the SAC (symmetry-adapted cluster)/SAC–CI (configuration interaction) method

Takahito Nakajima [a,b,c], Hiroshi Nakatsuji [a,b,c,*]

[a] *Department of Synthetic Chemistry and Biological Chemistry, Faculty of Engineering, Kyoto University, Sakyo-ku, Kyoto, 606-8501, Japan*

[b] *Department of Applied Chemistry, Graduate School of Engineering, University of Tokyo, Hongo, Tokyo, 113-0033, Japan*

[c] *Institute for Fundamental Chemistry, 34-4 Takano Nishi-Hiraki-cho, Sakyo-ku, Kyoto, 606-8103, Japan*

Received 18 May 1998

Abstract

A method for calculating the analytical energy gradient of the ground, excited, ionized, and electron-attached states calculated by the SAC (symmetry-adapted cluster)/SAC–CI (configuration interaction) method was formulated and implemented. This method adapts to the selection procedure of the linked and unlinked operators in the current SAC/SAC–CI code. It was applied to various molecules in various electronic states, and was confirmed to perform well for general use.

1. Introduction

The SAC (symmetry-adapted cluster)/SAC–CI (configuration interaction) method [1–3], which was originally reported in 1978 for studying the ground, excited, ionized, and electron-attached (anion) states, has been used in various studies of spectroscopies and chemical reactions of molecules [4,5], including surface–molecule interaction systems [6] and biochemical systems [7,8]. It has also been extended to high-spin states from quartet to septet spin multiplicities [9]. Based on the accumulated results of these studies, the SAC/SAC–CI method has been established as a powerful, computationally efficient, and reliable method for calculating ground and excited states of molecules in singlet to septet spin multiplicities.

The features of the current version of the SAC/SAC–CI code may be summarized as follows:

(1) The singlet closed-shell state is calculated by the SAC single-double (SD-*S*) method.

(2) Using the SAC–CI SD-*R* and general-*R* [10] methods, we can calculate the ground and excited states of singlet, triplet, ionized (doublet), electron-attached (doublet), quartet (ionized), quintet, sextet (ionized), and septet spin multiplicities. The SAC–CI SD-*R* method is suitable for ordinary one-electron

* Corresponding author. Department of Synthetic Chemistry and Biological Chemistry, Faculty of Engineering, Kyoto University, Sakyo-ku, Kyoto, 606-8501, Japan.

0301-0104/99/$ - see front matter
PII: S0301-0104(99)00004-X

processes like excitations and ionizations. The SAC–CI general-*R* method is useful for studying multi-electron processes, such as those involved in shake-up ionizations and in the excited A_g states of linear polyenes, and up to six-electron excited configurations are included in the linked operators.

(3) A neutral doublet radical, for example, is calculated by the SAC–CI method as a cationic state of a closed-shell anion or as an anionic state of a closed-shell cation. We can use the RHF orbitals of the neutral radical as reference molecular orbitals (MO).

(4) The properties of molecules in various electronic states are calculated from the SAC/SAC–CI wave functions: (i) density and spin–density matrices for the above states [11], (ii) one-electron properties for the above states [11], (iii) hyperfine splitting constants and cusp values of open-shell molecules [12,13], (iv) transition densities and transition moments among the above SAC/SAC–CI states [11], and (v) intensity of the ionization spectra [14,15].

(5) We can directly compare the energies and the properties of different electronic states calculated by the SAC/SAC–CI method. This is a very useful property when one studies the chemistry involving different electronic states.

Thus, the field of the SAC/SAC–CI method is certainly very wide: we can study chemistry and physics involved in many different states of singlet to septet spin multiplicities.

More recently, equation-of-motion coupled-cluster (EOM–CC) method was published by Bartlett group [16,17], but this method is essentially the same as the SAC–CI method, as noted previously in more detail in Ref. [18]. It is not based on the EOM method, which is an important methodology developed by Lowe [19], McKoy, Shibuya, and others [20–22], but is a minor modification of the already established SAC–CI method. The SAC/SAC–CI theory is exact. In practical calculations, we have to introduce some approximations. The differences between the two theories are only in the approximations adopted in the current codes.

The derivative of the energy with respect to the nuclear coordinate of a molecule gives fundamental information for investigating molecular geometry, vibration, chemical reaction, dynamics, etc. Furthermore, the derivative of the energy with respect to an external field, such as an electric or magnetic field, provides molecular properties, such as dipole moment, quadrupole moment, magnetic susceptibility, etc. Thus, the calculations of energy derivatives offer a useful and powerful tool for studying chemical reactions, dynamics and properties of molecules.

Two approaches have been developed for the energy gradient method; one uses the analytical energy gradient [23,24], and the other uses the Hellmann–Feynman force [25,26]. Though the Hellmann–Feynman theorem holds for exact and stable [27] wave functions, it is not satisfied for most approximate wave functions due to the linear combination of atomic orbital (LCAO)–molecular orbital (MO) approximations. Thus, the error term [28–31], which should be zero for exact and stable wave functions, is quite large for approximate wave functions. The Hellmann–Feynman theorem is useful for the plane wave basis (e.g., Car–Parrinello method [32,33]). For example, Nakatsuji proposed the Hellmann–Feynman force concept (electrostatic force (ESF) theory) for molecular geometries and chemical reactions [34–37]. This concept has been shown to be quite useful for predicting the geometries of molecules in ground and excited states. This concept further leads to the concept of electron-cloud preceding and incomplete following in chemical reactions and molecular vibrations [36]. Nakatsuji and coworkers [37] also reported a theorem which shows that there is a unique and systematic approach for improving the SCF and multi-configuration SCF (MC–SCF) wave functions so that they satisfy the Hellmann–Feynman theorem; a sufficient condition for the Hellmann–Feynman theorem to be satisfied is that the basis set includes the derivative for any basis included.

For the SAC–CI method, the Hellmann–Feynman theorem is not satisfied. Therefore, the analytical energy gradient method is necessary for the SAC–CI method. In this paper, we formulate and implement an SAC/SAC–CI energy gradient method which adapts to the perturbation selection scheme [15]. It would be useful to establish a systematic method for calculating the energy derivatives of excited states since molecules in excited states are generally very short-lived and it is difficult to observe the dynamics in excited states experimentally. A brief communication on this method has been reported previously

[38]. To the best of our knowledge, this is the first time that the energy gradient method has been implemented using the perturbation selection technique. The EOM–CC energy gradient [39–43], which is closely related to the SAC–CI gradient, has been developed by Stanton and Gauss: the method is straightforward in their integral-driven algorithm.

In this paper, we first briefly summarize the SAC/SAC–CI method that is pertinent to the present purpose. Next, we formulate the analytical gradients of the SAC and SAC–CI energies and describe the computational algorithm. We then apply this method to the various electronic states of several molecules. Finally, we give our conclusion in Section 4.

2. SAC / SAC–CI energy gradient method

2.1. Brief summary of the SAC / SAC–CI method

First, we briefly summarize the SAC/SAC–CI method. Reviews of the SAC/SAC–CI method have been published recently [4,5].

The SAC method is based on the spin and space symmetry-adapted formalism of the cluster expansion method [1]. The SAC wave function is described as the cluster expansion around the reference function $|0\rangle$, which is usually the Hartree–Fock (HF) single determinant,

$$|\Psi_{\mathrm{SAC}}\rangle = \exp(S)|0\rangle, \tag{1}$$

where

$$S = \sum_I C_I S_I^\dagger . \tag{2}$$

The operator $S_I^\dagger$ should be spin symmetry-adapted; otherwise, the wave function is not an eigen function of S^2. Actually, ordinary coupled-cluster (CC) wave functions are not eigen functions of S^2, just like the unrestricted Hartree–Fock (UHF) wave function. Using symmetry-adapted operators, the number of independent variables included in the cluster expansion is the same as that in the corresponding (symmetry-adapted) CI method. The difference between the SAC and ordinary CC expansions has been discussed previously [1].

The non-variational solution of the SAC wave function is obtained by left-projecting the Schrödinger equation for the SAC wave function onto the reference and linked excited configurations,

$$\langle 0|H - E_{\mathrm{SAC}}|\Psi_{\mathrm{SAC}}\rangle = 0, \tag{3}$$

and

$$\langle 0|S_K(H - E_{\mathrm{SAC}})|\Psi_{\mathrm{SAC}}\rangle = 0, \tag{4}$$

where H is the Hamiltonian and E_{SAC} is the SAC energy. The SAC method gives not only the accurate wave function for the ground state, but also the complementary functional space which spans the space for the excited states [2,3,5].

The SAC–CI wave function is described by taking a linear combination of these complementary functions [2,3,5], and is written essentially as

$$|\Psi^p_{\mathrm{SAC-CI}}\rangle = R^p|\Psi_{\mathrm{SAC}}\rangle, \tag{5}$$

where p denotes the pth state and

$$R^p = \sum_K d_K^p R_K^\dagger , \tag{6}$$

where $R_K^\dagger$ represents a set of excitation, ionization and/or electron-attachment operators, and d_K^p is the SAC–CI coefficient of the pth excited state. By considering Eq. (5), one notes that the SAC–CI method is based on the transferability of electron correlations between the ground and excited states. Since excitations and ionizations are only one- or two-electron processes, most of the electron correlations in the ground and excited states should be similar. It has been shown numerically that this transferability is quite satisfactory for ordinary one- and two-electron processes [4,5].

The non-variational SAC–CI (referred to as SAC–CI-NV) equation is obtained by projecting the Schrödinger equation for the SAC–CI wave function onto the space of the linked excited configurations,

$$\langle 0|R_K(H - E^p_{\mathrm{SAC-CI}})|\Psi^p_{\mathrm{SAC-CI}}\rangle = 0, \tag{7}$$

where $E^p_{\mathrm{SAC-CI}}$ is the SAC–CI energy of the pth state. Since Eq. (7) involves the diagonalization of non-symmetric matrices, we prepared an algorithm

for the iterative diagonalization of non-symmetric matrices [44], extending Davidson's procedure for symmetric matrices [45]. The left- and right-eigenvectors are denoted by $d^{\mathrm{L}p}$ and $d^{\mathrm{R}p}$, respectively. The SAC–CI wave function is described by the right eigenvectors, as seen in the definition given by Eqs. (5) and (6).

We can also use the approximately variational procedure for the SAC–CI method (referred to as the SAC–CI-V). In the SAC–CI-V method, the final matrices to be diagonalized are the symmetrized matrices of the SAC–CI-NV method. This method has also been shown to give satisfactory results [3,11], and has been used as a standard method.

2.2. Analytical gradients of the SAC energy

Our SAC/SAC–CI program code is Hamiltonian matrix-driven, as in the MR–CI codes, whereas almost all of the CC codes are integral-driven [46–53]. Therefore, we formulate the analytical gradients of the SAC and SAC–CI energies to be suitable for such an algorithm.

The approximations adopted in the following derivation are as follows; the linked terms in the SAC calculations include all single- (S_1) and selected double- (S_2) excitation operators, and the unlinked terms include quadruple-excitation operators as products of further selected double-excitation operators (S_2S_2) (referred to as SAC-A). The unlinked double S_1S_1 and triple S_1S_2 excitation operators are also included optionally. The SAC-Q and SAC-C [54] approximations are obtained by considering the $\langle 0|S_1HS_1^\dagger S_2^\dagger|0\rangle$ term, and the $\langle 0|S_1HS_1^\dagger S_2^\dagger|0\rangle$ and $\langle 0|S_2HS_1^\dagger S_2^\dagger|0\rangle$ terms, respectively. Under this approximation, the SAC equation is represented in Hamiltonian matrix form as

$$\begin{aligned}\Delta E_{\mathrm{SAC}} &= \sum_I C_I\langle 0|HS_I^\dagger|0\rangle \\ &\quad + \frac{1}{2}\sum_I\sum_J C_IC_J\langle 0|HS_I^\dagger S_J^\dagger|0\rangle \\ &\equiv \sum_I C_IH_{0I} + \frac{1}{2}\sum_I\sum_J C_IC_JH_{0,IJ}\,, \end{aligned} \tag{8}$$

and

$$\begin{aligned}&H_{K0} + \sum_I C_I(H_{KI} - \Delta E_{\mathrm{SAC}}S_{KI}) \\ &\quad + \frac{1}{2}\sum_I\sum_J C_IC_J(H_{K,IJ} - \Delta E_{\mathrm{SAC}}S_{K,IJ}) = 0\,, \end{aligned} \tag{9}$$

where $\Delta E_{\mathrm{SAC}} = E_{\mathrm{SAC}} - E_{\mathrm{HF}}$. Throughout this paper, we represent the Hamiltonian matrices $\langle 0|S_IHS_J^\dagger|0\rangle$ and $\langle 0|S_IHS_J^\dagger S_K^\dagger|0\rangle$ as H_{IJ} and H_{IJK}, respectively, and the overlap matrices between the configurations $\langle 0|S_IS_J^\dagger|0\rangle$ and $\langle 0|S_IS_J^\dagger S_K^\dagger|0\rangle$ as S_{IJ} and S_{IJK}, respectively. The unlinked $H_{0.IJ}$ and $S_{K.IJ}$ terms do not practically appear in Eqs. (8) and (9), respectively, since the disjoint $S_IS_J^\dagger$ excitation operator can be represented by the linked operator $S_K^\dagger$ if $S_{K.IJ}$ is non-zero.

The first derivative of the SAC correlation energy is derived by differentiating Eq. (8) with respect to the external parameter a, and is given as

$$\frac{\partial\Delta E_{\mathrm{SAC}}}{\partial a} = \sum_I C_I\bar{H}_{0I}^a + \sum_I C_I^a\bar{\bar{H}}_{0I}\,, \tag{10}$$

where

$$\bar{H}_{KI}^a \equiv \frac{\partial H_{KI}}{\partial a} + \frac{1}{2}\sum_J C_J\frac{\partial H_{K,IJ}}{\partial a}\,, \tag{11}$$

$$\bar{\bar{H}}_{KI} \equiv H_{KI} + \sum_J C_JH_{K,IJ}\,, \tag{12}$$

and

$$C_I^a \equiv \frac{\partial C_I}{\partial a}\,. \tag{13}$$

In this equation, we need information about the first derivative of the SAC coefficient $\partial C_I/\partial a$ since the SAC coefficients are not determined variationally, and this is determined by the coupled-perturbed SAC (CPSAC) equation which is obtained by differentiating the SAC equation (Eq. (9)) with respect to

a. The CPSAC equation is linear and is written in matrix form as

$$\boldsymbol{Y}\boldsymbol{C}^a = \boldsymbol{X}\,, \tag{14}$$

where the matrix $\boldsymbol{Y}$ and the vector $\boldsymbol{X}$ are given by

$$Y_{KI} \equiv \overline{\overline{H}}_{KI} - \Delta E_{\mathrm{SAC}}\bar{S}_{KI} - \left(\sum_J C_J \bar{S}_{KJ}\right)\overline{\overline{H}}_{0I}\,, \tag{15}$$

and

$$X_K \equiv -\left\{ H^a_{K0} + \sum_I C_I \bar{H}^a_{KI} - \left(\sum_I C_I \bar{S}_{KI}\right)\left(\sum_I C_I \bar{H}_{0I}\right)\right\}, \tag{16}$$

where

$$\bar{S}_{KI} \equiv S_{KI} + \frac{1}{2}\sum_J C_J S_{K,IJ}\,, \tag{17}$$

and

$$H^a_{KI} \equiv \frac{\partial H_{KI}}{\partial a}\,. \tag{18}$$

Here and hereafter, the derivative of the overlap matrix between configurations disappears because it is zero at the configuration level; molecular orbital orthonormality is guaranteed by the following relationship,

$$U^a_{ij} + s^a_{ij} + U^a_{ji} = 0\,, \tag{19}$$

which is obtained by differentiating the MO overlap matrix, s_{ij}, where

$$s^a_{ij} = \sum_{\mu\nu}^{AO} c_{\mu i} c_{\nu j} \frac{\partial(\mu|\nu)}{\partial a}\,, \tag{20}$$

and $c_{\mu i}$ is the coefficient of the μth atomic orbital χ_μ in the ith MO. The MO coefficient derivative, U^a_{ij}, is determined by the coupled-perturbed Hartree–Fock (CPHF) equation [23,24,55–57].

Explicit solution of the CPSAC equation is computationally costly, since $3N$ sets of unknowns, with N being the number of atoms, are required. However, this can be circumvented by using the interchange technique of Dalgarno and Stewart [58] (or the so-called $\boldsymbol{Z}$-vector method of Handy and Schaefer [59]). In the interchange technique, we introduce a new vector $\boldsymbol{Z}^{\mathrm{SAC}}$ (called the $\boldsymbol{Z}$-vector) defined by

$$\boldsymbol{Y}^T\boldsymbol{Z}^{\mathrm{SAC}} = \overline{\overline{H}}_0\,, \tag{21}$$

and the second term in Eq. (10) can then be rewritten in matrix form as

$$\overline{\overline{\boldsymbol{H}}}_0^T\boldsymbol{C}^a = \overline{\overline{\boldsymbol{H}}}_0^T\boldsymbol{Y}^{-1}\boldsymbol{X} = \left(\boldsymbol{Z}^{\mathrm{SAC}}\right)^T\boldsymbol{X}\,. \tag{22}$$

Thus, the first derivative of the SAC correlation energy given by Eq. (10) is rewritten as

$$\frac{\partial \Delta E_{\mathrm{SAC}}}{\partial a} = \sum_I C_I \bar{H}^a_{0I} + \sum_I X_I Z^{\mathrm{SAC}}_I\,. \tag{23}$$

An advantage of representing the first derivative of the SAC energy in Hamiltonian matrix form is that this derivative can be calculated even if we adopt the selection scheme for the operators $S^\dagger_I$ and $S^\dagger_I S^\dagger_J$. If we represent the energy in the integral-driven form at the beginning, we have to give up this selection scheme.

The Hamiltonian matrix element H_{IJ} is written as

$$H_{IJ} = \sum_{ij}^{MO} \gamma^{IJ}_{ij} f_{ij} + \sum_{ijkl}^{MO} \Gamma^{JJ}_{ijkl}(ij|kl)\,, \tag{24}$$

where γ^{IJ}_{ij} and Γ^{IJ}_{ijkl} are one- and two-electron coupling constants between the configuration functions Φ_I and Φ_J, f_{ij} is the Fock matrix element, and $(ij|kl)$ is the two-electron MO integral. Since the coupling constants are independent of the parameter a, the derivative of the Hamiltonian matrix is written as

$$\frac{\partial H_{IJ}}{\partial a} = \sum_{ij}^{MO} \gamma^{IJ}_{ij}\frac{\partial f_{ij}}{\partial a} + \sum_{ijkl}^{MO} \Gamma^{IJ}_{ijkl}\frac{\partial(ij|kl)}{\partial a}\,, \tag{25}$$

By using Eq. (25), Eq. (23) is rewritten as

$$\frac{\partial \Delta E_{\mathrm{SAC}}}{\partial a} = \sum_{ij}^{MO} \gamma^{\mathrm{SAC}}_{ij}\frac{\partial f_{ij}}{\partial a} + \sum_{ijkl}^{MO} \Gamma^{\mathrm{SAC}}_{ijkl}\frac{\partial(ij|kl)}{\partial a} \tag{26}$$

in a MO representation, where ΔE is the SAC or SAC–CI correlation energy, f_{ij} is the Fock matrix element, and $(ij|kl)$ is the two-electron MO integral.

γ_{ij} and Γ_{ijkl} are the SAC or SAC–CI one- and two-electron (1e and 2e) effective density matrices (EDM), respectively, in the MO representation, and are given by

$$\gamma_{ij}^{\mathrm{SAC}} \equiv \sum_I \left\{ \left(1 + \sum_J \sum_K Z_K^{\mathrm{SAC}} C_J \bar{S}_{KJ} \right) C_I - Z_I^{\mathrm{SAC}} \right\} \gamma_{ij}^{0I} - \sum_K \sum_I Z_K^{\mathrm{SAC}} C_I \bar{\gamma}_{ij}^{KI} , \tag{27}$$

and

$$\Gamma_{ijkl}^{\mathrm{SAC}} \equiv \sum_I \left(1 + \sum_J \sum_K Z_K^{\mathrm{SAC}} C_J \bar{S}_{KJ} \right) C_I \bar{\Gamma}_{ijkl}^{0I} - \sum_I Z_I^{\mathrm{SAC}} \Gamma_{ijkl}^{0I} - \sum_K \sum_I Z_K^{\mathrm{SAC}} C_I \bar{\Gamma}_{ijkl}^{KI} , \tag{28}$$

where

$$\bar{\gamma}_{ij}^{KI} \equiv \gamma_{ij}^{KI} + \frac{1}{2} \sum_J C_J \gamma_{ij}^{K,IJ} , \tag{29}$$

and

$$\bar{\Gamma}_{ijkl}^{KI} \equiv \Gamma_{ijkl}^{KI} + \frac{1}{2} \sum_J C_J \Gamma_{ijkl}^{K,IJ} , \tag{30}$$

Eq. (26) gives the first derivative of the SAC energy in the MO representation. As will be shown in Section 2.3, the first derivative of the SAC–CI energy has the same form as that of the SAC one, that is, the sum of the one- and two-electron parts. Before we rewrite the first derivative of the SAC energy in the AO representation, we derive the MO representation of the first derivative of the SAC–CI energy in Section 2.3.

2.3. Analytical gradients of the SAC–CI energy

As mentioned above, the EOM–CC method is theoretically similar to the SAC–CI method, although an integral-driven form is used in the actual calculations. The present SAC–CI gradient method uses a Hamiltonian matrix-driven algorithm in contrast to the EOM–CC gradient method presented by Stanton [39–43].

Using Eq. (7), the SAC–CI-NV energy is written as

$$\Delta E_{\mathrm{SAC-CI}}^{p} = \sum_M \sum_N d_M^{\mathrm{L}\,p} d_N^{\mathrm{R}\,p} \bar{\bar{H}}_{MN} , \tag{31}$$

where $\Delta E_{\mathrm{SAC-CI}}^{p} = E_{\mathrm{SAC-CI}}^{p} - E_{\mathrm{HF}}$, and $d_M^{\mathrm{L}\,p}$ and $d_N^{\mathrm{R}\,p}$ are, respectively, left- and right-vector coefficients of the pth solution the SAC–CI Eq. (7). We adopt the convention that the subscripts I, J, K, and L refer to the SAC excitation operators, while M and N refer to the SAC–CI excitation operators. Furthermore, the eigenvector biorthonormalization condition is given by

$$\sum_M \sum_N d_M^{\mathrm{L}\,p} d_N^{\mathrm{R}\,p} \bar{\bar{S}}_{MN} = \delta_{pq} , \tag{32}$$

where

$$\bar{\bar{S}}_{MN} \equiv S_{MN} + \sum_I C_I S_{M,NI} . \tag{33}$$

Hereafter, we are interested only in the pth state of the SAC–CI solutions, and therefore do not give the superscript p in the following equations. By differentiating Eq. (31), the first derivative of the SAC–CI correlation energy with respect to the external parameter a is written as

$$\frac{\partial \Delta E_{\mathrm{SAC-CI}}}{\partial a} = \sum_M \sum_N \frac{\partial d_M^{\mathrm{L}}}{\partial a} d_N^{\mathrm{R}} \bar{\bar{H}}_{MN} + \sum_M \sum_N d_M^{\mathrm{L}} \frac{\partial d_N^{\mathrm{R}}}{\partial a} \bar{\bar{H}}_{MN} + \sum_M \sum_N d_M^{\mathrm{L}} d_N^{\mathrm{R}} \bar{\bar{H}}_{MN}^{a} + \sum_M \sum_N \sum_I d_M^{\mathrm{L}} d_N^{\mathrm{R}} \frac{\partial C_I}{\partial a} H_{M,NI} , \tag{34}$$

where

$$\bar{\bar{H}}_{MN}^{a} \equiv \frac{\partial H_{MN}}{\partial a} + \sum_I C_I \frac{\partial H_{M,NI}}{\partial a} . \tag{35}$$

The derivative of the SAC–CI coefficient is eliminated by using the SAC–CI equation, Eq. (7), and the biorthonormalization condition, Eq. (32), and we obtain,

$$\frac{\partial \Delta E_{\mathrm{SAC-CI}}}{\partial a} = \sum_M \sum_N \mathrm{d}_M^{\mathrm{L}} \mathrm{d}_N^{\mathrm{R}} \bar{\bar{H}}_{MN}^{a} + \sum_I \mathrm{C}_I^{a} \bar{\bar{\boldsymbol{H}}}_{\mathrm{I}}, \tag{36}$$

where

$$\bar{\bar{\boldsymbol{H}}}_{\mathrm{I}} \equiv \sum_M \sum_N \mathrm{d}_M^{\mathrm{L}} \mathrm{s}_N^{\mathrm{R}} \left(H_{M,NI} - \Delta E_{\mathrm{SAC-CI}} S_{M,NI} \right). \tag{37}$$

We note that information regarding the derivative of the SAC coefficient is necessary in the last term of Eq. (36), and may be calculated using the CPSAC equation. However, this again can be avoided by using the interchange technique for the SAC–CI case. Introducing the SAC–CI $\boldsymbol{Z}$-vector $\boldsymbol{Z}^{\mathrm{SAC-CI}}$ defined by

$$\boldsymbol{Y}^{\mathrm{T}} \boldsymbol{Z}^{\mathrm{SAC-CI}} = \bar{\bar{\mathbf{H}}}, \tag{38}$$

the first derivative of the SAC–CI energy can be written as

$$\frac{\partial \Delta E_{\mathrm{SAC-CI}}}{\partial a} = \sum_M \sum_N d_M^{\mathrm{L}} d_N^{\mathrm{R}} \bar{\bar{H}}_{MN}^{a} + \sum_I X_I Z_I^{\mathrm{SAC-CI}}. \tag{39}$$

As in the case of the SAC energy gradient, we rewrite Eq. (39) in the MO integral form as

$$\frac{\partial \Delta E_{\mathrm{SAC-CI}}}{\partial a} = \sum_{ij}^{MO} \gamma_{ij}^{\mathrm{SAC-CI}} \frac{\partial f_{ij}}{\partial a} + \sum_{ijkl}^{MO} \Gamma_{ijkl}^{\mathrm{SAC-CI}} \frac{\partial (ij|kl)}{\partial a}, \tag{40}$$

where the SAC–CI 1e and 2e MO–EDMs are represented as

$$\gamma_{ij}^{\mathrm{SAC-CI}} \equiv \sum_I \left\{ \left(\sum_J \sum_K Z_K^{\mathrm{SAC-CI}} C_J \bar{S}_{KJ} \right) C_I - Z_I^{\mathrm{SAC-CI}} \right\} \gamma_{ij}^{0I} + \sum_M \sum_N d_M^{\mathrm{L}} d_N^{\mathrm{R}} \bar{\bar{\gamma}}^{MN} - \sum_K \sum_I Z_K^{\mathrm{SAC-CI}} C_I \bar{\gamma}_{ijkl}^{KI}, \tag{41}$$

and

$$\Gamma_{ijkl}^{\mathrm{SAC-CI}} \equiv \sum_I \left\{ \left(\sum_J \sum_K Z_K^{\mathrm{SAC-CI}} C_J \bar{S}_{KJ} \right) C_I - Z_I^{\mathrm{SAC-CI}} \right\} \Gamma_{ijkl}^{0I} + \sum_M \sum_N d_M^{\mathrm{L}} d_N^{\mathrm{R}} \bar{\bar{\Gamma}}_{ijkl}^{MN} - \sum_K \sum_I Z_K^{\mathrm{SAC-CI}} C_I \bar{\Gamma}_{ijkl}^{KI}, \tag{42}$$

respectively, and where

$$\bar{\bar{\gamma}}_{ij}^{MN} \equiv \gamma_{ij}^{MN} + \sum_I C_I \gamma_{ij}^{M,NI}, \tag{43}$$

and

$$\bar{\bar{\Gamma}}_{ijkl}^{MN} \equiv \Gamma_{ijkl}^{MN} + \sum_I C_I \Gamma_{ijkl}^{M,NI}. \tag{44}$$

We also implement the first derivative of the approximately variational SAC–CI (SAC–CI-V) energy. This implementation is straightforward since the SAC–CI-V method is obtained simply by symmetrizing the SAC–CI-NV matrices.

2.4. Evaluation of SAC / SAC–CI energy gradient

In Sections 2.2 and 2.3, we derived the MO representations of the first derivatives of the SAC and SAC–CI energies, which involve the derivatives of the MO Fock matrices and the 2e MO integrals. We know that the 2e AO derivative integrals are mostly zero since only such derivative integrals that include the AOs whose centers are involved in the derivative calculation are non-zero, while the MO derivative integrals are generally non-zero. Therefore, the MO representation of the derivative integrals is not effective or practical. Thus, instead of transforming the derivative integrals, we back-transform the effective density matrix from MO to AO representation [60]. In this section, we rewrite the first derivatives of the SAC and SAC–CI energies from MO to AO representation.

The first derivatives of the Fock matrix and the two-electron integrals included in Eqs. (26) and (40) are rewritten as

$$\frac{\partial f_{ij}}{\partial a} = f_{ij}^{a} + \sum_m^{MO} \left(U_{mi}^{a} f_{mj} + U_{mj}^{a} f_{im} \right), \tag{45}$$

and

$$\frac{\partial(ij|kl)}{\partial a} = (ij|kl)^a + \sum_m^{MO} \{U^a_{mi}(mj|kl) + U^a_{mj}(im|kl) + U^a_{mk}(ij|ml) + U^a_{ml}(ij|km)\}, \quad (46)$$

respectively, where f^a_{ij} and $(ij|kl)^a$ are the skeleton derivatives [23] defined by

$$f^a_{ij} = h^a_{ij} + \sum_k^{d.o.} \{2(ij|kk)^a - (ik|jk)^a\}, \quad (47)$$

and

$$(ij|kl)^a = \sum_{\mu\nu\rho\sigma}^{AO} c_{\mu i}c_{\nu j}c_{\rho k}c_{\sigma l}\frac{\partial(\mu\nu|\rho\sigma)}{\partial a}, \quad (48)$$

respectively, where h^a_{ij} is the core Hamiltonian derivative,

$$h^a_{ij} = \sum_{\mu\nu}^{AO} c_{\mu i}c_{\nu j}\frac{\partial(\mu|h|\nu)}{\partial a}. \quad (49)$$

The MO coefficient derivative, U^a_{mi}, is obtained by solving the CPHF equation [23,24,55–57].

Using Eqs. (45) and (46), the first derivative of the SAC or SAC–CI energy given by Eq. (26) or Eq. (40) is written as

$$\frac{\partial \Delta E}{\partial a} = \sum_{ij}^{MO} \gamma_{ij} f^a_{ij} + \sum_{ijkl}^{MO} \Gamma_{ijkl}(ij|kl)^a + 2\sum_m^{MO}\sum_i^{MO} U^a_{mi}\left\{\sum_j^{MO} \gamma_{ij} f_{mj} + 2\sum_{jkl}^{MO} \Gamma_{ijkl}(mj|kl)\right\}. \quad (50)$$

The first two terms of Eq. (50) are rewritten by back-transforming the effective density matrix from MO representation to AO representation as,

$$\frac{\partial \Delta E}{\partial a} = \sum_{\mu\nu}^{AO} \gamma_{\mu\nu}\frac{\partial f_{\mu\nu}}{\partial a} + \sum_{\mu\nu\rho\sigma}^{AO} \Gamma_{\mu\nu\rho\sigma}\frac{\partial(\mu\nu|\rho\sigma)}{\partial a} + 2\sum_m^{MO}\sum_i^{MO} U^a_{mi}\left\{\sum_i^{MO} \gamma_{ij} f_{mj} + 2\sum_{jkl}^{MO} \Gamma_{ijkl}(mj|kl)\right\}. \quad (51)$$

The explicit solution of the derivative of the MO coefficient, U^a_{mi}, can be avoided by using the interchange technique [58,59], as explained for the SAC coefficient.

2.5. Algorithm

The SAC/SAC–CI energy gradient code has been implemented into the SAC85 [61] and SAC–CI96 [62] program systems in the SD-*R* approximation. In addition, the gradients of the CIS (singles), CISD (singles and doubles), MP2 (second-order Møller–Plesset perturbation), and SACD (SAC doubles) energies have also been implemented. The basic algorithm is as follows:

(1) The SCF calculation is performed and the derivatives of the one- and two-electron AO integrals are calculated using the GAUSSIAN 94 [63] or HONDO8 [64] program package.

(2) The SAC and SAC–CI calculations are carried out, and the information on the configurations selected is stored to be used in a later step.

(3) The CPSAC $\boldsymbol{Z}$-vector equations (Eq. (21) or Eq. (38)) and the CPHF $\boldsymbol{Z}$-vector equations are solved using Pulay's direct inversion in the iterative subspace (DIIS) method [65]. The DIIS method is also useful for solving the SAC equation.

(4) The SAC and SAC–CI MO effective density matrices given, respectively, by Eqs. (27) and (28) and by Eqs. (41) and (42) are constructed and stored.

(5) The SAC and SAC–CI energy gradients are calculated using Eq. (51). The explicit solution of the derivative of the MO coefficient, as well as the SAC coefficient, is avoided by using the interchange technique [58,59]. In this step, we perform the back-transformation of the effective density matrix from the MO basis to the AO basis.

The linked terms in the SAC calculations include all single- (S_1) and selected double- (S_2) excitation operators. The unlinked terms are included in different ways in the SAC–CI96 program [62]. In the standard applications, we use the SAC-A approximation (see Section 2.2), in which selected quadruple-excitation operators which are the products of the double-excitation operators (S_2S_2) are included as the unlinked terms. In the standard SAC–CI calculations, the linked term includes all of the single- (R_1) and selected double- (R_2) excitation operators, and

the unlinked term includes the disjoint triple-excitation operators (R_1S_2).

A numerical check of the implemented program was carried out by comparing the present results with those obtained by numerical differentiations.

2.6. GSUM method

A feature of the present SAC/SAC–CI energy gradient code is that it adapts to the perturbation selection scheme used in the SAC/SAC–CI calculations. This will make the calculation of truly large molecules possible. However, for example in the geometry optimization, the independent selection of operators at independent geometries may lead to a discontinuity of the potential surface. To avoid this discontinuity, we adopt the GSUM method [66], which was previously applied to calculations of the potential energy curves of Li_2 [66].

The geometry optimization using the GSUM method is summarized as follows. Before optimization, we choose representative points which cover the reaction coordinate under consideration and take the group sum of the linked and unlinked operators selected by the ordinary method [15] for all the representative points in the nuclear configuration space. Geometry optimization is performed within this configuration space. The usefulness of this method has been confirmed by previous applications [38,66].

3. Applications

3.1. Diatomic molecules – without selection

As an application of the present SAC/SAC–CI energy gradient method, we first calculate the spectroscopic constants of the ground and excited states of the diatomic molecules LiH, BH, BeH, and CH without the perturbation selection scheme. The experimental data for the equilibrium internuclear distance r_e, harmonic vibrational frequency ω_e, and adiabatic transition energy T_e of these diatomic molecules have been reported previously [67]. We calculate the equilibrium internuclear distances and harmonic vibrational frequencies using the SAC/SAC–CI energy gradient method, and evaluate the adiabatic transition energies. The singlet and triplet states are calculated for LiH and BH, and the doublet states are calculated for BeH and CH. The singlet ground states are determined by the SAC energy gradient method, and the other excited states are determined by the SAC–CI energy gradient method. The doublet states are obtained by the ionizations of the corresponding anionic closed-shell molecules or by electron attachment of the corresponding cationic closed-shell molecules. The SAC–CI calculations are performed using both the non-variational and approximate variational methods (SAC–CI-NV and SAC–CI-V, respectively).

The basis sets used for LiH, BeH, and CH are the 6-311 + + G^{**} sets [68,69], and that for BH is the Huzinaga–Dunning (9s5p/4s)/[4s2p/2s] set [70,71] augmented with polarization and diffuse functions; for boron, the orbital exponent of the sp diffuse function is 0.0315 and the exponent of the d polarization function is 0.7. For hydrogen, the exponent of the s diffuse function is 0.036 and the exponent of the p polarization function is 1.0.

The calculated results for these diatomic molecules are shown in Table 1, and are compared with experimental findings [67]. The results calculated by the SAC/SAC–CI energy gradient method are generally consistent with the experimental findings. The differences in the equilibrium distances between the SAC/SAC–CI and experimental results are within 0.015 Å, and those in the harmonic vibrational frequencies are within about 60 cm^{-1}. The adiabatic transition energies fall within about 0.25 eV of the experimental values.

The results obtained by the SAC–CI-V method are very close to those obtained by the SAC–CI-NV method. The adiabatic transition energies calculated by the SAC–CI-V method are generally a little smaller than those calculated by the SAC–CI-NV method. The differences in the equilibrium distances between SAC–CI-NV and SAC–CI-V are within a few 10^{-4} Å. Thus, the SAC–CI-V method is useful for calculating excited states.

In Table 1, we compare r_e and ω_e of the ground state of BeH calculated by the SAC–CI ionization and electron-attachment methods applied to the BeH^- and BeH^+ closed-shell states, respectively.

Table 1
Equilibrium internuclear distances, harmonic vibrational frequencies, and adiabatic transition energies

Molecule	State	Method	Equilibrium internuclear distance r_e (Å)	Harmonic vibrational frequency ω_e (cm^{-1})	Adiabatic transition energy T_e (eV)
LiH	$X^1\Sigma^+$	SAC	1.5948	1394	0.0
		experimental[a]	1.5957	1406	0.0
	$B^1\Pi$	SAC–CI-NV	2.3788	261	4.2193
		SAC–CI-V	2.3788	263	4.2192
		experimental[a]	2.378	–	4.3285
	$b^3\Pi$	SAC–CI-NV	1.9895	592	4.0242
		SAC–CI-V	1.9895	592	4.0241
BH	$X^1\Sigma^+$	SAC	1.2397	2376	0.0
		experimental[a]	1.2324	2367	0.0
	$a^3\Pi$	SAC–CI-NV	1.1933	2660	1.2322
		SAC–CI-V	1.1940	2654	1.2305
	$A^1\Pi$	SAC–CI-NV	1.2321	2263	3.1252
		SAC–CI-V	1.2330	2249	3.1224
		experimental[a]	1.2186	2251	6.2848
		SAC–CI-V	1.2435	1655	6.2820
	$B^1\Sigma^+$	SAC–CI-NV	1.2178	2423	6.4742
		SAC–CI-V	1.2181	2425	6.4710
		experimental[a]	1.2164	2400	6.4888
BeH	$X^2\Sigma^+$	SAC–CI-NV[b]	1.3389	2096	0.0
		SAC–CI-V[b]	1.3390	2107	0.0
		SAC–CI-NV[c]	1.3470	2075	0.0
		SAC–CI-V[c]	1.3470	2069	0.0
		experimental[a]	1.3426	2061	0.0
	$A^2\Pi_r$	SAC–CI-NV[b]	1.3344	2099	2.5609
		SAC–CI-V[b]	1.3346	2095	2.5598
		experimental[a]	1.3336	2089	2.4838
	$B^2\Pi$	SAC–CI-NV[b]	1.3120	2255	6.4597
		SAC–CI-V[b]	1.3179	2194	6.4590
		experimental[a]	1.3092	2266	6.3086
CH	$X^2\Pi_r$	SAC–CI-NV[b]	1.1218	2923	
		SAC–CI-V[b]	1.1222	2921	
		experimental[a]	1.1199	2859	

[a] Ref. [67].
[b] Obtained by electron attachment from BeH^+ or CH^+.
[c] Obtained by ionization from BeH^-.

The SCF orbitals used are those for an anion or cation instead of a neutral radical, since the CPHF method we have coded is currently limited to closed shells. Nevertheless, the two results agree well with each other. The equilibrium distance calculated by the electron-attached SAC–CI method is smaller by about 0.008 Å than that calculated by the ionized SAC–CI method, while the harmonic vibrational frequency calculated by the electron-attached SAC–CI method is larger by 20–40 cm^{-1}. The main reason for these differences lies in the difference in the HF orbitals used.

3.2. Diatomic molecules – with the GSUM method

To demonstrate the performance of the GSUM method in the selection scheme, we calculate the equilibrium internuclear distance r_e and adiabatic transition energy T_e of the diatomic molecules BF and NO. For NO, we previously studied the excita-

tion and ionization spectra by the SAC/SAC–CI method [72].

The basis set for BF is the 6-311++G** set [68,69]. The basis set for NO is the Huzinaga–Dunning (9s5p)/[4s2p] set [70,71] augmented with polarization and diffuse functions; for oxygen, the exponents of the s and p diffuse functions are 0.032 and 0.028, respectively, and the exponent of the d polarization function is 0.85. For nitrogen, the exponents of the s and p diffuse functions are 0.023 and 0.021, respectively, and the exponent of the d polarization function is 0.8.

The singlet ground state of BF is calculated by the SAC energy gradient method. The excited singlet and triplet states of BF and the ground and excited doublet states of NO are calculated by the SAC–CI energy gradient method. The doublet states of NO are obtained by electron attachment of the corresponding closed-shell cation NO^+. The SAC–CI calculations for BF are performed by the SAC–CI-NV method, and those for NO are performed by the SAC–CI-V method.

Energy thresholds of 1×10^{-5} and 1×10^{-7} hartree are used for the ground and excited states, respectively, in the perturbation selection scheme. Geometry optimization is performed as follows: perturbation selection is performed with the experimental geometry and geometry optimization is performed while maintaining this selected space. Although the experimental geometries are used for perturbation selection, other choices, such as the optimized geometries at the HF/CIS level, may also be used, since we have found that the dependence on this choice is small. For the $E^2\Sigma^+$ state of NO, selection was performed at 1.08 Å since the experimental value could not be found.

The calculated results for BF and NO in Table 2 are comparable to experimental findings [67]. The results calculated by the SAC/SAC–CI energy gradient method are generally consistent with the exper-

Table 2
Equilibrium internuclear distances and adiabatic transition energies

Molecule	State	Method	Equilibrium transition distance r_e (Å)	Adiabatic transition energy T_e (eV)
BF	$X^1\Sigma^+$	SAC–CI	1.265	0.0
		experimental[a]	1.263	0.0
	$a^3\Pi$	SAC–CI	1.319	3.547
		experimental[a]	1.308	3.613
	$A^1\Pi$	SAC–CI	1.315	6.643
		experimental[a]	1.304	6.343
	$b^3\Sigma^+$	SAC–CI	1.213	7.778
		experimental[a]	1.215	7.567
	$B^1\Sigma^+$	SAC–CI	1.204	8.539
		experimental[a]	1.207	8.103
NO	$X^2\Pi$	SAC–CI	1.165	0.0
		experimental[a]	1.151	0.0
	$A^2\Sigma^+$	SAC–CI	1.077	5.054
		experimental[a]	1.063	5.451
	$C^2\Pi$	SAC–CI	1.074	6.094
		experimental[a]	1.062	6.463
	$D^2\Sigma^+$	SAC–CI	1.077	6.144
		experimental[a]	1.062	6.582
	$E^2\Sigma^+$	SAC–CI	1.085	7.425
		experimental[a]	–	7.517
	$H'^2\Pi$	SAC–CI	1.075	7.654
		experimental[a]	1.059	7.747

[a] Ref. [67].

imental values. This shows that the SAC/SAC–CI energy gradient method is also effective and useful when the perturbation selection scheme is used.

3.3. CH_2 and SiH_2

We next studied the singlet–triplet energy separations of CH_2 and SiH_2 molecules. It is well known that the ground state of CH_2 is $^3B_1$ and the first excited state is $^1A_1$, while this is reversed for SiH_2. Many theoretical and experimental studies have been published for CH_2 [73–80] and SiH_2 [77,81,82].

Two basis sets are used for CH_2. The first basis set (Basis I) is the Huzinaga–Dunning (9s5p/4s)/[4s2p/2s] set [70,71] augmented with the carbon d ($\zeta = 0.74$ for $^3B_1$ and 0.51 for $^1A_1$) and hydrogen p ($\zeta = 1.0$) polarization functions, which has often been used to calculate the singlet–triplet energy separation of CH_2 [75,78]. Using this basis set and the experimental geometries, we previously calculated the singlet–triplet energy separation for the ground and excited states by the SAC method, and obtained a reasonable value of 11.8 kcal/mol [75]. The second basis set (Basis II) is the same as that used by Beärda et al. [80], and is larger than Basis I. The basis set for SiH_2 is the same as the f basis referred to by Balasubramanian and McLean [81].

For CH_2, the results for Basis I and II are shown in Table 3. No perturbation selection was performed in these calculations. For Basis I, we perform the SAC-A, SAC-Q and SAC-C calculations and the corresponding SAC–CI-NV calculations. The different SAC/SAC–CI calculations give similar geometries, dipole moments, and singlet–triplet energy separations. The SAC–CI-V and -NV results based on SAC-A are again very close to each other.

Here, we want to see how well-balanced the SAC/SAC–CI results for the singlet and triplet states are in comparison with the results of the UHF-based CC method. The UHF-based CC result is spin-contaminated, while the SAC/SAC–CI result is spin-pure. Comparable QCISD calculations [83] were performed, using the same basis sets, by the GAUSSIAN 94 program [63] as a UHF-based CC method. For the geometric parameters, the results obtained by the SAC/SAC–CI method are similar to those obtained by the UHF-based QCISD method. However, the singlet–triplet energy separation differs by more than 1 kcal/mol, and the SAC/SAC–CI result is closer than the UHF-based QCISD result

Table 3
Total energies, geometries, singlet–triplet energy separation, and dipole moments of CH_2 (Basis I and II)

State	Method	Total energy (a.u.)	CH (Å)	HCH (deg.)	Separation (kcal/mol)	Dipole moment (D)
Basis I						
1^1A_1	SAC-A	−39.038193	1.118	101.66	0.0	−1.858
	SAC-Q	−39.038267	1.118	101.55	0.0	−1.856
	SAC-C	−39.038244	1.118	101.66	0.0	−1.856
1^3B_1	SAC–CI-NV(SAC-A)	−39.057491	1.082	132.21	−12.11	−0.660
	SAC–CI-V(SAC-A)	−39.057620	1.082	132.25	−12.19	−0.659
	SAC–CI-NV(SAC-Q)	−39.057500	1.082	132.24	−12.07	−0.660
	SAC–CI-V(SAC-C)	−39.057492	1.082	132.24	−12.08	−0.660
	QCISD[a]	−39.059454	1.082	132.42	−13.30	−0.669
	experimental[b]		1.0766 ± 0.0014	134.037 ± 0.045	−9.272 ± 0.03	
Basis II						
1^1A_1	SAC-A	−39.048908	1.112	101.36	0.0	−1.689
	SAC-Q	−39.049002	1.112	101.28	0.0	−1.686
1^3B_1	SAC–CI-NV	−39.065057	1.082	132.21	−10.13	−0.587
	SAC–CI-V	−39.065212	1.082	132.21	−10.23	−0.586
	QCISD[a]	−39.067297	1.082	132.29	−11.48	−0.593
	experimental[b]		1.0766 ± 0.0014	134.037 ± 0.045	−9.272 ± 0.03	

[a] Present UHF-based calculation by GAUSSIAN 94. $\langle S^2 \rangle = 2.015$ for both Basis I and II.
[b] Ref. [82].

Table 4
Total energies, geometries, singlet–triplet energy separation, and dipole moments of SiH_2

State	Method	Total energy (a.u.)	SiH (Å)	HSiH (deg.)	Separation (kcal/mol)	Dipole moment (D)
1^3B_1	SAC–CI-NV	−290.2 26602	1.489	117.43	0.0	+0.007
1^1A_1	SAC-A	−290.2 62293	1.513	93.83	−22.40	−0.384
	experi mental[c]		1.516_3	92.8	-21.0 ± 0.7, -18.0 ± 0.7	

[a]Ref. [82].

to the experimental value [73,74]. This result is common to both basis sets and shows that the SAC/SAC–CI method gives well-balanced descriptions for different spin–multiplet states because it is free from spin-contamination.

The result for SiH_2 is shown in Table 4. Perturbation selections with energy thresholds of 1×10^{-5} and 1×10^{-6} hartree were performed for the ground and excited states, respectively. The configuration spaces throughout the geometry optimization were fixed to those selected at the $^1A_1$ and $^3B_1$ HF optimized geometries. The results for the geometric parameters agree well with the experimental findings. The singlet–triplet energy separation calculated by the SAC/SAC–CI method is −22.40 kcal/mol, which is consistent with the experimental value of $-21.0\ (\pm 0.7)$ kcal/mol [82] as well as with previous theoretical results [78,81].

3.4. C_2H_4

Molecular ethylene in the ground and excited states has been extensively studied both experimentally and theoretically [84]. We previously [84,85] calculated the electronic spectrum of ethylene by the SAC/SAC–CI method, and the results agreed very well with experimental findings. Here, we calculate the equilibrium geometries for ethylene in the ground and excited states by the SAC/SAC–CI energy gradient method.

Foresman et al. [86] calculated the CIS optimized geometries at the 6-31 + G* basis [87–89] for the $^1B_{1u}$, $^3B_{1u}$, and $^1B_{3u}$ states. We used the same basis set for the sake of comparison. Energy thresholds of 1×10^{-5} and 1×10^{-7} hartree are used for the ground and excited states, respectively, in the perturbation selection scheme. Selection is performed at the CIS optimized geometries reported by Foresman et al. [86], and these selected spaces are fixed throughout the geometry optimization. For comparison, optimization was performed for the $^1B_{3u}$ state using the GSUM space of those selected at the experimental [90] and CIS optimized geometries.

Table 5 shows the result for the optimized geometries in the ground and excited states of ethylene. Although the differences between the HF/CIS and SAC/SAC–CI methods are small, the results obtained by the SAC/SAC–CI method are closer to the experimental findings [90,91]. For the $^1B_{3u}$ state, which is the 3s Rydberg state, both the CIS [86] and SAC–CI methods predict a planar D_{2h} geometry, while a D_2 structure (azimuthal angle of 37.0°) has been reported experimentally [90]. The MR (multi-

Table 5
Equilibrium geometries in the ground and excited states of ethylene

State	Method	Point group	CC (Å)	CH (Å)	CCH (deg.)
Ground	HF	D_{2h}	1.321	1.076	121.73
	SAC	D_{2h}	1.334	1.083	121.81
	experimental[a]	D_{2h}	1.337	1.084	121.25
$^1B_{1u}$ (V)	CIS[b]	D_{2d}	1.376	1.090	123.74
	SAC–CI	D_{2d}	1.364	1.101	124.46
$^3B_{1u}$ (T)	CIS[b]	D_{2d}	1.461	1.076	121.30
	SAC–CI	D_{2d}	1.462	1.085	121.16
$^1B_{3u}$ (3s)	CIS[b]	D_{2h}	1.413	1.071	120.36
	SAC–CI[c]	D_{2h}	1.411	1.082	120.52
	SAC–CI[d]	D_{2h}	1.413	1.083	120.58
	experimental[e]	D_2^f	1.41	1.08	117.8

[a]Ref. [91].
[b]Ref. [86].
[c]Configuration selection was performed with the CIS optimized geometry.
[d]Configuration selection was performed by the GSUM method for the CIS optimized and experimental geometries.
[e]Ref. [90].
[f]The azimuthal angle is 37.0°.

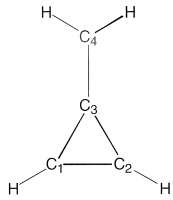

Fig. 1.

reference) D–CI result reported by Petrongolo et al. [92], which was obtained by optimizing only the azimuthal angle, predicted a non-planar D_2 geometry. This implies that further examination is necessary from both theoretical and experimental perspectives. Furthermore, we see for this state that the difference due to the difference in the selection procedure is very small. This confirms the usefulness of the GSUM method.

3.5. Methylenecyclopropene

In the ultraviolet (UV) spectrum of methylenecyclopropene (Fig. 1), Staley and Norden [93] observed three peaks which they assigned using the semi-empirical INDO/S–CI method [94]. The first peak at 206 nm, which shows strong solvent-dependence, was assigned to the $^1B_2$ transition, and the second (at 242 nm) and third (at 309 nm) peaks were assigned to the $^1B_1$ and $^1A_1$ transitions, respectively. The CIS calculation [95] also supports these assignments. Norden et al. [96] also reported the experimental and theoretical structures and dipole moment for the ground state. We calculate here the equilibrium geometries and the dipole moments of methylenecyclopropene in the ground and excited states using the SAC/SAC–CI energy gradient method.

The 6-31G* basis [68,69] used in the previous MP2 calculation [96] is adopted for the sake of comparison. Energy thresholds of 1×10^{-5} and 1×10^{-7} hartree were used for the ground and excited states, respectively, in the perturbation selection scheme. Perturbation selections were performed at the following geometries: the MP2 optimized geometry [96] for the ground state, the CIS optimized geometries for the singlet and triplet excited states, and the UHF optimized geometries for the cationic and anionic states. These CIS and UHF geometries are shown for comparison in Table 6. The vertical excitation energies and dipole moments were calculated using the SAC optimized geometries in the ground state with a better-quality 6-31++G** basis [87–89].

Table 6 shows the SAC/SAC–CI optimized geometries for the ground, singlet and triplet excited, ionized, and electron-attached states. The previous theoretically optimized and experimental geometries [96] are also shown for comparison. The SAC result for the ground state is very similar to the MP2 and experimental results [96]. All of the excited, ionized and electron-attached states calculated in Table 6 mainly involve the highest-occupied (HO) and lowest-unoccupied (LU) MOs. The HOMO has its largest amplitude at C_4 and shows C_1C_2 π-bonding and C_3C_4 π-bonding nature, and a node exists between

Table 6
Equilibrium geometries in the ground, excited, ionized, and anionized states of methylenecyclopropene

	Ground			Singlet		Triplet		Cation		Anion	
	SAC	MP2[a]	Experimental[a,b]	SAC–CI	CIS	SAC–CI	CIS	SAC–CI	UHF	SAC–CI	UHF
C_1C_2	1.320	1.326	1.323	1.501	1.481	1.511	1.501	1.352	1.341	1.434	1.418
C_1C_3	1.445	1.445	1.441	1.352	1.350	1.405	1.416	1.381	1.364	1.421	1.407
C_3C_4	1.329	1.330	1.332	1.426	1.397	1.354	1.325	1.413	1.421	1.365	1.363
C_1H	1.077	1.080	(1.080)	1.071	1.062	1.070	1.063	1.073	1.071	1.068	1.067
C_4H	1.076	1.083	(1.085)	1.081	1.071	1.075	1.074	1.075	1.072	1.078	1.078
C_2C_1H	148.20	148.1	(147.5)	152.18	151.66	151.07	151.00	149.47	149.45	151.51	151.21
HC_4H	118.86	118.0	(118.0)	116.98	118.73	117.39	117.60	120.44	120.54	117.61	117.91

[a] Ref. [96].
[b] Experimental geometries were obtained under the assumption that the geometric parameters involving the hydrogen atoms were fixed at the values given in parentheses.

Table 7
Excitation energies and dipole moments of methylenecyclopropene

State	Excitation energy(eV)			Dipole moment (D)		
	HF/CIS[a]	SAC/SAC–CI	Experimental[b]	HF/CIS[a]	SAC/SAC–CI	Experimental[c]
Ground	0.0	0.0	0.0	−2.391	−1.988	-1.90 ± 0.2
$^1B_2$	5.508	4.810	4.01	+2.598	+2.344	–
$^1B_1$	5.462	5.365	5.12	−3.155	−0.957	–
$^1A_2$	6.031	5.924	–	−1.205	+1.916	–
$^1B_1$	6.128	5.957	–	+3.858	+0.175	–
$^1A_1$	6.416	6.311	6.02	−1.369	−1.506	–

[a] Present calculation.
[b] Ref. [93].
[c] Ref. [96].

these bonds. The LUMO has C_1C_2 π-antibonding nature. The structural changes in all of the calculated states are well interpreted by these natures of the HOMO and LUMO.

The excitation energies and dipole moments calculated by the SAC/SAC–CI method are listed in Table 7, and are compared with those obtained by the HF/CIS method and experimentally. The excitation energies calculated by the SAC/SAC–CI method are closer to the experimental values. For the lowest $^1B_2$ excited state, the deviation is still as large as 0.8 eV. The reason for this may lie in the strong solvent-dependence mentioned above, which is certainly caused by a large change in the dipole moment between the ground and excited states. The dipole moment of the ground state calculated by the SAC method is improved, and close to the experimental value. Furthermore, we note that the dipole moments of the two $^1B_1$ and $^1A_2$ excited states are quite different between the SAC–CI and CIS calculations, in comparison with those in the $^1B_2$ and $^1A_1$ states.

4. Conclusions

An analytical energy gradient method for the ground, excited, ionized, and electron-attached states calculated by the SAC/SAC–CI method was formulated and implemented in the SAC85 [61] and SAC–CI96 [62] programs. This method adapts to the perturbation selection technique used in our SAC/SAC–CI code. This is the first such implementation for the excited states and is easily applied to the MR–CI code. The reliability and usefulness of the present method were confirmed, based on its application to various molecules in the ground and excited states. We are currently combining the present code with the HF SCF program to make it more efficient for studying the dynamics and properties of molecules in the ground, excited, ionized, and electron-attached states.

The present SAC/SAC–CI energy gradient method can be easily extended to the high-spin SAC–CI [6] and general-*R* SAC–CI [10] methods, and we are currently performing such implementations.

Acknowledgements

We would like to thank Kyoto University–Venture Business Laboratory. One of the authors (TN) thanks Japan Society for the Promotion of Science for financial support. This study was supported in part by a Grant-in-Aid for Scientific Research from the Ministry of Education, Science and Culture and by the New Energy and Industrial Technology Development Organization (NEDO).

References

[1] H. Nakatsuji, K. Hirao, J. Chem. Phys. 68 (1978) 2053.
[2] H. Nakatsuji, Chem. Phys. Lett. 59 (1978) 362.
[3] H. Nakatsuji, Chem. Phys. Lett. 67 (1979) 329, 334.

[4] H. Nakatsuji, Acta Chim. Hung. 129 (1992) 719.
[5] H. Nakatsuji, in: J. Leszczynski (Ed.), Computational Chemistry – Reviews of Current Trends, Vol. 2, World Scientific, 1997, p. 62.
[6] H. Nakatsuji, Prog. Surf. Sci. 54 (1997) 1, and references cited therein.
[7] H. Nakatsuji, J. Hasegawa, M. Hada, J. Chem. Phys. 104 (1996) 2321.
[8] Y. Tokita, H. Nakatsuji, J. Phys. Chem. B 101 (1997) 3281, and references cited therein.
[9] H. Nakatsuji, M. Ehara, J. Chem. Phys. 98 (1993) 7179.
[10] H. Nakatsuji, Chem. Phys. Lett. 177 (1991) 331.
[11] H. Nakatsuji, K. Hirao, Int. J. Quantum Chem. 20 (1981) 1301.
[12] H. Nakatsuji, K. Ohta, T. Yonezawa, J. Phys. Chem. 87 (1983) 3068.
[13] H. Nakatsuji, M. Ehara, T. Momose, J. Chem. Phys. 100 (1994) 5821.
[14] H. Nakatsuji, T. Yonezawa, Chem. Phys. Lett. 87 (1982) 426.
[15] H. Nakatsuji, Chem. Phys. 75 (1983) 425.
[16] J. Geetsen, M. Rittby, R.J. Bartlett, Chem. Phys. Lett. 164 (1989) 57.
[17] J.F. Stanton, R.J. Bartlett, J. Chem. Phys. 98 (1993) 7029.
[18] H. Nakatsuji, M. Ehara, J. Chem. Phys. 101 (1994) 7658.
[19] D.J. Rowe, Rev. Mod. Phys. 40 (1968) 153.
[20] T. Shibuya, V. McKoy, Phys. Rev. A 2 (1970) 2208.
[21] J. Rose, T. Shibuya, V. McKoy, J. Chem. Phys. 58 (1973) 74.
[22] D. Yeager, V. McKoy, G.A. Segal, J. Chem. Phys. 61 (1974) 755.
[23] Y. Yamaguchi, Y. Osamura, J.D. Goddard, H.F. Schaefer, A New Dimension to Quantum Chemistry: Analytic Derivative Methods in ab initio Molecular Electronic Structure Theory, Oxford, New York, 1994.
[24] P. Jørgensen, J. Simons (Eds.), Geometrical Derivatives of Energy Surfaces and Molecular Properties, Reidel, Dordrecht, 1986.
[25] H. Hellmann, Einführung in die Quantenchemie, Deuticke, Leipzig, 1937, p. 285.
[26] R.P. Feynman, Phys. Rev. 56 (1936) 340.
[27] A.C. Harley, Proc. R. Soc. London, Ser. A 226 (1954) 170.
[28] H. Nakatsuji, K. Kanda, T. Yonezawa, Chem. Phys. Lett. 75 (1980) 340.
[29] H. Nakatsuji, T. Hayakawa, M. Hada, Chem. Phys. Lett. 80 (1981) 94.
[30] H. Nakatsuji, K. Kanda, T. Yonezawa, J. Chem. Phys. 77 (1982) 3109.
[31] H. Nakatsuji, K. Kanda, in: J. Avery, J.P. Dahl (Eds.), Local Density in Quantum Chemistry and Solid State Theory, Plenum Press, New York, 1982.
[32] R. Car, M. Parrinello, Phys. Rev. Lett. 55 (1985) 2471.
[33] Y. Imamura, Y. Morikawa, T. Yamasaki, H. Nakatsuji, Surf. Sci. Comm. 341 (1995) L1091.
[34] H. Nakatsuji, J. Am. Chem. Soc. 95 (1973) 345, 354, 2084, 6894
[35] H. Nakatsuji, J. Am. Chem. Soc. 96 (1974) 6000.
[36] H. Nakatsuji, J. Am. Chem. Soc. 96 (1974) 24, 30.
[37] H. Nakatsuji, in: B.M. Deb (Ed.), The Force Concept in Chemistry, Van Nostrand, Princeton, NJ, 1981.
[38] T. Nakajima, H. Nakatsuji, Chem. Phys. Lett. 280 (1997) 79.
[39] J.F. Stanton, J. Chem. Phys. 99 (1993) 8840.
[40] J.F. Stanton, J. Gauss, J. Chem. Phys. 100 (1994) 4695.
[41] J.F. Stanton, J. Gauss, J. Chem. Phys. 101 (1994) 8938.
[42] J.F. Stanton, J. Gauss, Theor. Chim. Acta 91 (1995) 267.
[43] J.F. Stanton, R.J. Bartlett, J. Chem. Phys. 98 (1993) 7029.
[44] K. Hirao, H. Nakatsuji, J. Comp. Phys. 45 (1982) 246.
[45] E.R. Davidson, J. Comp. Phys. 17 (1975) 87.
[46] P. Jørgensen, J. Simons, J. Chem. Phys. 79 (1983) 334.
[47] L. Adamowicz, W.D. Laidig, R.J. Bartlett, Int. J. Quantum Chem. (Symp.) 18 (1984) 245.
[48] G. Fitzgerald, R.J. Harisson, W.D. Laidig, R.J. Bartlett, Chem. Phys. Lett. 117 (1985) 433.
[49] G. Fitzgerald, R.J. Harisson, R.J. Bartlett, J. Chem. Phys. 85 (1986) 5143.
[50] A.C. Scheiner, G.E. Scuseria, J.E. Rice, T.J. Lee, H.F. Schaefer III, J. Chem. Phys. 87 (1987) 5361.
[51] J. Gauss, D. Cremer, Chem. Phys. Lett. 150 (1988) 280.
[52] J. Gauss, D. Cremer, Chem. Phys. Lett. 163 (1989) 549.
[53] J. Gauss, D. Cremer, Adv. Quantum Chem. 23 (1992) 205.
[54] K. Hirao, Y. Hatano, Chem. Phys. Lett. 100 (1983) 519.
[55] J. Gerratt, I.M. Mills, J. Chem. Phys. 49 (1968) 1719.
[56] J.A. Pople, R. Krishnan, H.B. Schlegel, J.S. Binkley, Int. J. Quantum Chem. (Symp.) 13 (1979) 225.
[57] N.C. Handy, R.D. Amos, J.F. Gaw, J.E. Rice, E.D. Simandiras, Chem. Phys. Lett. 120 (1985) 151.
[58] A. Dalgarno, A.L. Stewart, Proc. R. Soc. A 247 (1958) 245.
[59] N.C. Handy, H.F. Schaefer III, J. Chem. Phys. 81 (1984) 5031.
[60] J.E. Rice, R.D. Amos, Chem. Phys. Lett. 138 (1987) 131.
[61] H. Nakatsuji, Program System for SAC and SAC–CI calculations, Program Library No. 146 (Y4/SAC) Data Processing Center of Kyoto University, 1985; H. Nakatsuji, Program Library SAC85 (No. 1396) Computer Center of the Institute for Molecular Science, Okazaki, Japan, 1986.
[62] H. Nakatsuji, M. Hada, M. Ehara, J. Hasegawa, T. Nakajima, H. Nakai, O. Kitao, K. Toyota, SAC/SAC–CI program system (SAC–CI96) for calculating ground, excited, ionized, and electron-attached states having singlet to septet spin multiplicities, 1996.
[63] GAUSSIAN94 (revision B3), M.J. Frisch, G.W. Trucks, H.B. Schlegel, P.M.W. Gill, B.G. Johnson, M.A. Robb, J.R. Cheeseman, T.A. Keith, G.A. Petersson, J.A. Montgomery, K. Raghavachari, M.A. Al-Laham, V.G. Zakrzewski, J.V. Ortiz, J.B. Foresman, J. Cioslowski, B.B. Stefanov, A. Nanayakkara, M. Challacombe, C.Y. Peng, P.Y. Ayala, W. Chen, M.W. Wong, J.L. Andres, E.S. Replogle, R. Gomperts, R.L. Martin, D.J. Fox, J.S. Binkley, D.J. Defrees, J. Baker, J.P. Stewart, M. Head-Gordon, C. Gonzalez, and J.A. Pople, Gaussian, Pittsburgh, PA, 1995.
[64] M. Dupuis, S.A. Maluendes, in: E. Clementi (Ed.), MOTECC Modern Techniques in Computational Chemistry 1991, ESCOM Science Publ., Leiden, 1991.
[65] P. Pulay, Chem. Phys. Lett. 73 (1980) 393.

[66] H. Nakatsuji, J. Ushio, T. Yonezawa, Can. J. Chem. 63 (1985) 1857.
[67] K.P. Huber, G. Herzberg, Molecular Spectra and Molecular Structure, IV. Constants of Diatomic Molecules, Van Nostrand, New York, 1979.
[68] R. Krishnan, J.S. Binkley, R. Seeger, J.A. Pople, J. Chem. Phys. 72 (1980) 650.
[69] A.D. McLean, G.S. Chandler, J. Chem. Phys. 72 (1980) 5639.
[70] S. Huzinaga, J. Chem. Phys. 42 (1965) 1293.
[71] T.H. Dunning Jr., J. Chem. Phys. 53 (1970) 2823.
[72] H. Nakatsuji, Int. J. Quantum Chem. (Symp.) 17 (1983) 241.
[73] P.R. Bunker, in: R.J. Bartlett (Ed.), Comparison of ab initio Quantum Chemistry with Experiment for Small Molecules, Reidel, Dordrecht, 1985, p. 141.
[74] P.R. Bunker, P. Jensen, W.P. Kraemer, R. Beardsworth, J. Chem. Phys. 85 (1986) 3724.
[75] K. Hirao, H. Nakatsuji, Chem. Phys. Lett. 79 (1981) 292.
[76] S.J. Cole, G.D. Purvis III, R.J. Bartlett, Chem. Phys. Lett. 113 (1985) 271.
[77] Ch.W. Bauschlicher Jr., P.R. Taylor, J. Chem. Phys. 85 (1986) 6510.
[78] Ch.W. Bauschlicher Jr., S.R. Langhoff, P.R. Taylor, J. Chem. Phys. 87 (1987) 387.
[79] A. Balková, R.J. Bartlett, J. Chem. Phys. 102 (1995) 7116.
[80] R.A. Beärda, M.C. van Hemert, E.F. van Dishoeck, J. Chem. Phys. 97 (1992) 8240.
[81] K. Balasubramanian, A.D. McLean, J. Chem. Phys. 85 (1986) 5117.
[82] J. Berkowitz, J.P. Greene, H. Cho, B. Ruscic, J. Chem. Phys. 86 (1987) 1235.
[83] J.A. Pople, M. Head-Gordon, K. Raghavachari, J. Chem. Phys. 87 (1987) 5968.
[84] C.C. Ballard, M. Hada, H. Nakatsuji, Bull. Chem. Soc. Jpn 69 (1996) 1901, and references therein.
[85] H. Nakatsuji, J. Chem. Phys. 80 (1984) 3703.
[86] J.B. Foresman, M. Head-Gordon, J.A. Pople, M.J. Frisch, J. Phys. Chem. 96 (1992) 135.
[87] W.J. Hehre, R. Ditchfield, J.A. Pople, J. Chem. Phys. 56 (1972) 2257.
[88] M.J. Frisch, J.A. Pople, J.S. Binkley, J. Chem. Phys. 80 (1984) 3265.
[89] T. Clark, J. Chandrasekhar, G.W. Spitznagel, P.v.R. Schleyer, J. Comput. Chem. 4 (1983) 294.
[90] P.D. Foo, K.K. Innes, J. Chem. Phys. 60 (1974) 4582.
[91] G. Herzberg, Electronic Spectra and Electronic Structure of Polyatomic Molecules, Van Nostrand, New York, 1966.
[92] C. Petrongolo, R.J. Buenker, S.D. Peyerimhoff, J. Chem. Phys. 76 (1982) 3655.
[93] S.W. Staley, T.D. Norden, J. Am. Chem. Soc. 106 (1984) 3699.
[94] G. Buemi, A. Raudino, F. Zuccarello, THEOCHEM 1 (1981) 285.
[95] J.B. Foresman, Æ. Frisch, Exploring Chemistry with Electronic Structure Methods, 2nd edn., Gaussian, Pittsburgh, PA, 1996.
[96] T.D. Norden, S.W. Staley, W.H. Taylor, M.D. Harmony, J. Am. Chem. Soc. 108 (1986) 7912.